1975

Flight director laws for the longitudinal cyclic and collective controls of the UH-1H helicopter.

Smith, Gordon Kenneth

Monterey, California. Naval Postgraduate School

FLIGHT DIRECTOR LAWS FOR THE LONGITUDINAL CYCLIC AND COLLECTIVE CONTROLS OF THE UH-1H HELICOPTER

Gordon Kenneth Smith

NAVAL POSTGRADUATE SCHOOL
Monterey, California

THESIS

FLIGHT DIRECTOR LAWS FOR THE
LONGITUDINAL CYCLIC AND COLLECTIVE CONTROLS
OF THE UH-1H HELICOPTER

by

Gordon Kenneth Smith

March 1975

Thesis Advisor: Ronald A. Hess

SECURITY CLASSIFICATION OF THIS PAGE (When Data Entered)

REPORT DOCUMENTATION PAGE		READ INSTRUCTIONS BEFORE COMPLETING FORM
1. REPORT NUMBER	2. GOVT ACCESSION NO.	3. RECIPIENT'S CATALOG NUMBER
4. TITLE (and Subtitle) Flight Director Laws for the Longitudinal Cyclic and Collective Controls of the UH-1H Helicopter		5. TYPE OF REPORT & PERIOD COVERED Master's Thesis March 1975
		6. PERFORMING ORG. REPORT NUMBER
7. AUTHOR(s) Gordon Kenneth Smith		8. CONTRACT OR GRANT NUMBER(s)
9. PERFORMING ORGANIZATION NAME AND ADDRESS Naval Postgraduate School Monterey, California 93940		10. PROGRAM ELEMENT, PROJECT, TASK AREA & WORK UNIT NUMBERS
11. CONTROLLING OFFICE NAME AND ADDRESS Naval Postgraduate School Monterey, California 93940		12. REPORT DATE March 1975
		13. NUMBER OF PAGES
14. MONITORING AGENCY NAME & ADDRESS(if different from Controlling Office)		15. SECURITY CLASS. (of this report)
		15a. DECLASSIFICATION/DOWNGRADING SCHEDULE

16. DISTRIBUTION STATEMENT (of this Report)

Approved for public release; distribution unlimited.

17. DISTRIBUTION STATEMENT (of the abstract entered in Block 20, if different from Report)

18. SUPPLEMENTARY NOTES

19. KEY WORDS (Continue on reverse side if necessary and identify by block number)

20. ABSTRACT (Continue on reverse side if necessary and identify by block number)

A technique for determining flight director laws for the longitudinal control of a V/STOL aircraft in landing approach is evaluated. The method is based on the application of an optimal control model for the human pilot. The vehicle studied was the UH-1H helicopter at three approach groundspeeds: 60 knots, 40 knots, and 20 knots. The two pilot outputs were longitudinal cyclic and collective. In the analysis, ten pilot

DD FORM 1 JAN 73 1473 EDITION OF 1 NOV 65 IS OBSOLETE
(Page 1) S/N 0102-014-6601 |

SECURITY CLASSIFICATION OF THIS PAGE (When Data Entered)

"transfer functions" which relate the two control variables to the five displayed and perceived quantities were obtained. These transfer functions were then utilized to obtain the respective flight director laws.

Flight Director Laws for the Logitudinal

Cyclic and Collective Controls of the UH-1H Helicopter

by

Gordon Kenneth Smith
Lieutenant, United States Navy
B.S., United States Naval Academy, 1968

Submitted in partial fulfillment of the
requirements for the degree of

MASTER OF SCIENCE IN AERONAUTICAL ENGINEERING

from the

NAVAL POSTGRADUATE SCHOOL
March 1975

ABSTRACT

A technique for determining flight director laws for the longitudinal control of a V/STOL aircraft in landing approach is evaluated. The method is based on the application of an optimal control model for the human pilot. The vehicle studied was the UH-1H helicopter at three approach groundspeeds: 60 knots, 40 knots, and 20 knots. The two pilot outputs were longitudinal cyclic and collective. In the analysis, ten pilot "transfer functions" which relate the two control variables to the five displayed and perceived quantities were obtained. These transfer functions were then utilized to obtain the respective flight director laws.

TABLE OF CONTENTS

LIST OF TABLES

LIST OF FIGURES

ACKNOWLEDGEMENTS

I wish to thank Dr. Ronald Hess, under whose supervision I worked, for his assistance and patience during the preparation of this thesis. Thanks is also due my wife, Glenna, for her confidence and assurance throughout this project.

I. INTRODUCTION

VTOL aircraft have received considerable attention for both military and civilian use, due to their unique ability to operate in areas not accessible to conventional aircraft. The rotary-wing aircraft, in particular, has shown such increased diversity that display systems which will allow VTOL operations in zero/zero conditions are being actively sought. Well-designed flight directors are the heart of such systems.

A flight director is a display system which provides control commands to the pilot to enable him to complete demanding flight tasks with relative ease and precision. Recently, Levison [Ref. 1] has proposed an analytical technique for flight director design based upon the optimal pilot model pioneered by Kleinman, Baron, and Levison [Ref. 2]. A modified form of this technique is utilized in this thesis to obtain the longitudinal flight director laws for the UH-1H helicopter in three approach conditions in the presence of random vertical and horizontal atmospheric turbulence. Five vehicle motion quantities, which are normally directly displayed or perceived by the pilot, are blended to drive two display symbols, the cyclic director and the collective director. The design was undertaken at three different groundspeeds: 60 knots, 40 knots, and 20 knots. The pilot-vehicle system for the optimal modeling procedure is shown graphically in Figure 1.

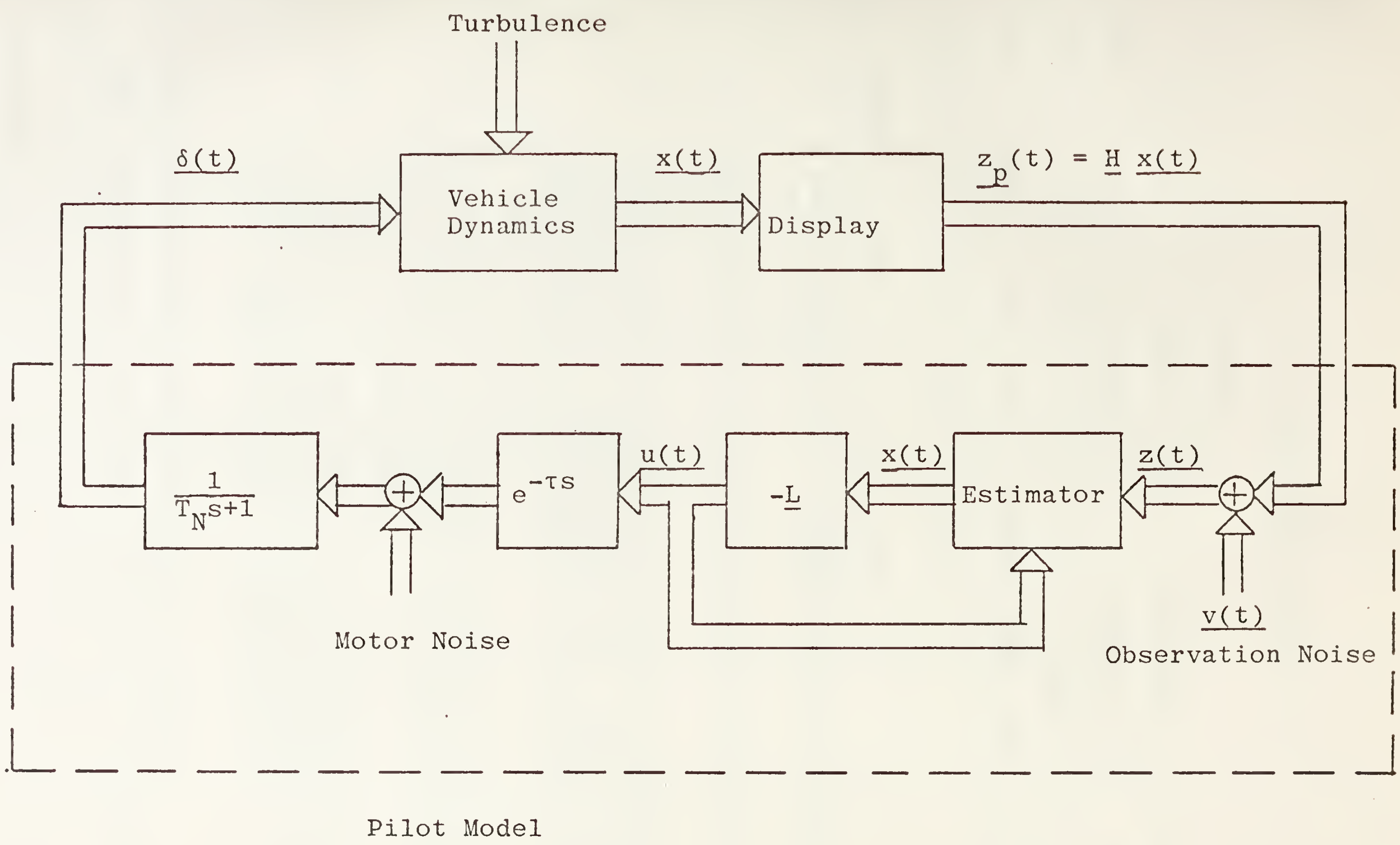

FIGURE 1. PILOT - VEHICLE SYSTEM MODEL

II. METHOD OF ANALYSIS

A. THE MODELING HYPOTHESIS

Subject to his inherent limitations, the well-trained, well motivated pilot behaves in an optimal manner. The pilot's control characteristics can be modeled by the solution of an optimal linear control problem and an optimal estimation problem with certain "modifications."

B. MODIFICATIONS FOR PILOT MODELING

1. A pure time delay is included in each of the pilot's control outputs.

2. Each output neuromuscular system is modeled as a first order lag.

3. Each observed variable is assumed to contain pilot induced additive white noise which scales with the variance of the observed variable. Also, each control output is assumed to contain pilot induced additive white noise which scales with the variance of the control motion.

4. If a variable is displayed explicitly, the pilot also perceives the first derivative of the variable but no higher derivatives. The first derivative is also noise contaminated.

5. The index of performance for the optimization procedure is chosen subjectively to mirror what the display system designer believes to be the task and control objectives perceived by the pilot.

C. LONGITUDINAL HELICOPTER EQUATIONS OF MOTION

The longitudinal helicopter equations of motion are shown in state variable form on the next page. The assumptions used in the derivation of these equations follow

$$\dot{u} = X_u u + X_w w + X_q q - g\theta + X_{\delta_B}\delta_B + X_{\delta_C}\delta_C - X_u u_g - X_w w_g \tag{1}$$

$$\dot{w} = z_u u + z_w w + (U_o + z_q)q + z_{\delta_B}\delta_B + z_{\delta_C}\delta_C - z_u u_g - z_w w_g \tag{2}$$

$$\begin{aligned}\dot{q} = {} & (M_u + M_{\dot{w}} z_u)u + (M_w + M_{\dot{w}} z_w)w + \left[M_q + M_{\dot{w}}(U_o + z_q) \right] q + (M_{\delta_B} + M_{\dot{w}} z_{\delta_B})\delta_B \\ & + (M_{\delta_C} + M_{\dot{w}} z_{\delta_C})\delta_C - (M_u + M_{\dot{w}} z_u)u_g - (M_w + M_{\dot{w}} z_w)w_g\end{aligned} \tag{3}$$

$$\dot{\theta} = q \tag{4}$$

$$\dot{h} = -w + U_o\theta \tag{5}$$

1. The vehicle is idealized as a rigid airframe to which is attached a rotor.

2. The rotor is described by the tip path plane whose orientation determined propulsive and aerodynamic forces and moments.

3. No rotor degrees of freedom are considered other than control inputs which serve to describe instantaneous tip path plane orientation.

4. All coupling between longitudinal and lateral motion is ignored.

5. There is linearized small perturbation motion about the horizontal reference flight path.

D. ATMOSPHERIC TURBULENCE

The power spectral densities for the atmospheric turbulence are those suggested by Hart, Adkins, and Lacau /Ref. 3/.

$$\Phi_{w_g w_g}(\omega) = \frac{2\sigma_w^2 L_w}{U_o} \left(\frac{1}{1 + (\frac{L_w \omega}{U_o})^2} \right) \tag{6}$$

$$\Phi_{u_g u_g}(\omega) = \frac{2\sigma_u^2 L_u}{U_o} \left(\frac{1}{1 + (\frac{L_u \omega}{U_o})^2} \right) \tag{7}$$

with

$$\alpha_1 = \sqrt{\frac{2U_o}{L_w}}\ \sigma_w \qquad\qquad \beta_1 = \frac{U_o}{L_w} \tag{8}$$

$$\alpha_2 = \sqrt{\frac{2U_o}{L_u}}\ \sigma_u \qquad\qquad \beta_2 = \frac{U_o}{L_u} \tag{9}$$

Using the concept of a white noise excited shaping filter, the following state equations can be developed.

$$\dot{w}_g = -\beta_1 w_g + \alpha_1 v_1 \tag{10}$$

$$\dot{u}_g = -\beta_2 u_g + \alpha_2 v_2 \tag{11}$$

Equations (10) and (11) now augment equations (1) - (5).

E. NEUROMUSCULAR AND TIME DELAY EQUATIONS

As noted in section II.B., a pure time delay and first ordger lag are included in the pilot's output. The delay is approximated by a second-order Pade' function. The quality of first and second order Pade' approximations are indicated in Figure 2 for the frequency interval of interest in pilot modeling, $\omega\tau < 5$ RAD. For ease of development, a portion of Figure 1 is shown here.

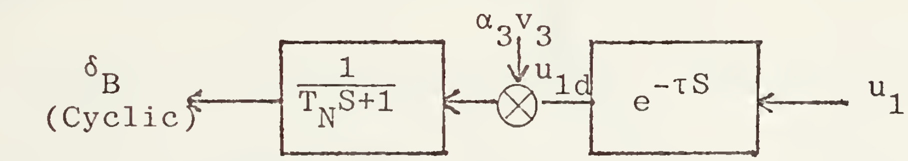

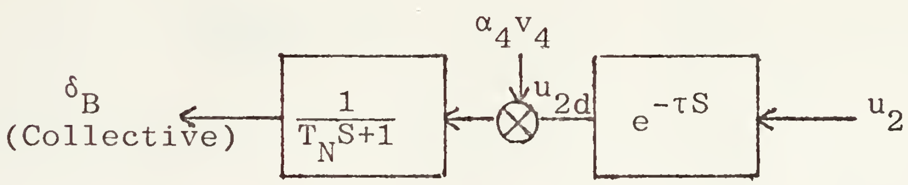

where $\alpha_3 v_3$ and $\alpha_4 v_4$ are motor noise

$$e^{-\tau s} \doteq \frac{(s-4/\tau)^2}{(s+4/\tau)^2} = \frac{\bar{u}_{1d}}{\bar{u}_1} = \frac{\bar{u}_{2d}}{\bar{u}_2} \tag{12}$$

or

$$\ddot{u}_{1d} + \frac{8}{\tau}\dot{u}_{1d} + \frac{16}{\tau^2}u_{1d} = \ddot{u}_1 - \frac{8}{\tau}\dot{u}_1 + \frac{16}{\tau^2}u_1 \tag{13}$$

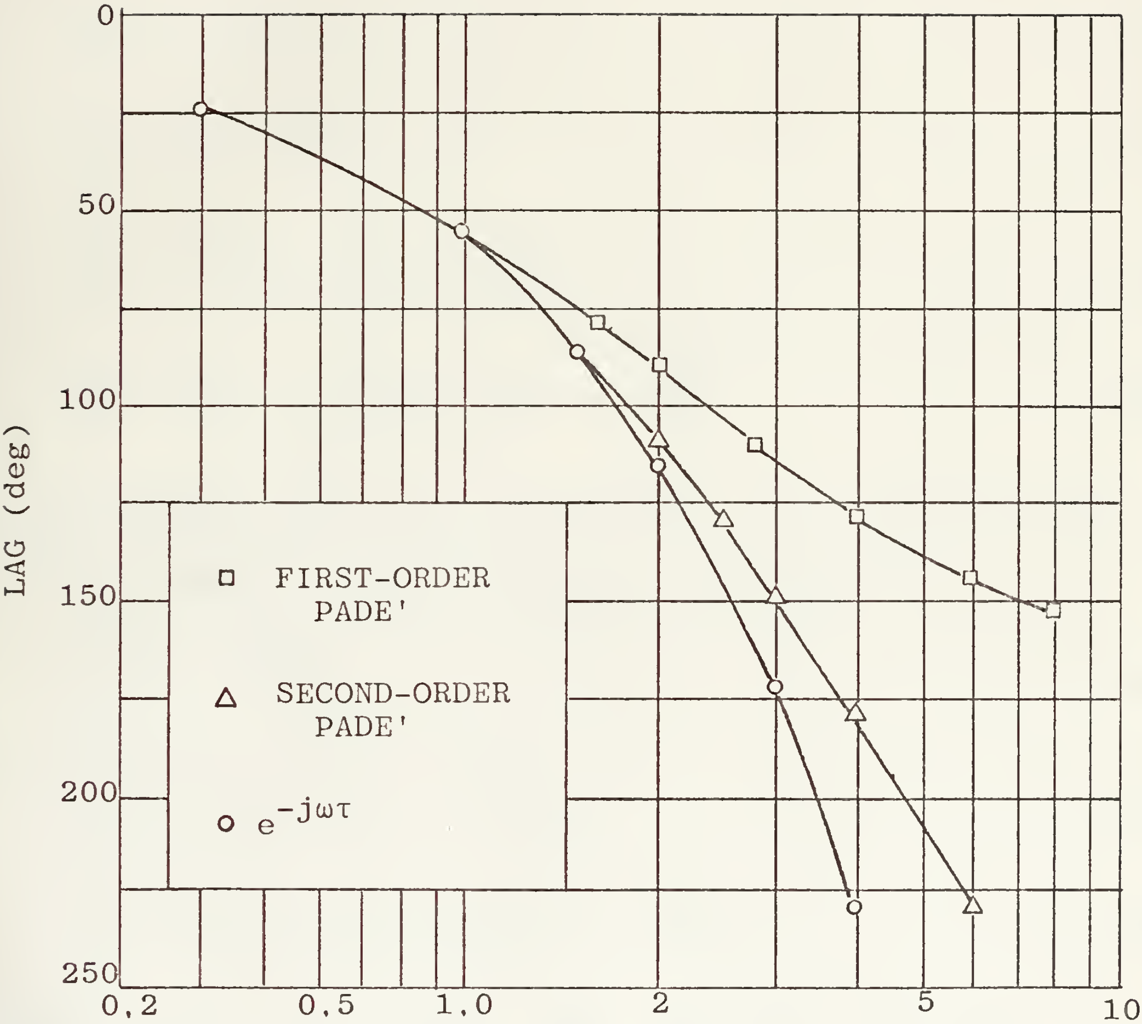

FIGURE 2. PADE' COMPARISONS

$$\ddot{u}_{2d} + \frac{8}{\tau}\dot{u}_{2d} + \frac{16}{\tau^2}u_{2d} = \ddot{u}_2 - \frac{8}{\tau}\dot{u}_2 + \frac{16}{\tau^2}u_2 \tag{14}$$

Now let

$$d_1 = u_{1d} - u_1 \tag{15}$$

$$d_2 = \dot{d}_1 + \frac{16}{\tau}u_1 \tag{16}$$

$$\dot{d}_1 = d_2 - \frac{16}{\tau}u_1 \tag{17}$$

$$\dot{d}_2 = -\frac{16}{\tau^2}d_1 - \frac{8}{\tau}d_2 + \frac{128}{\tau^2}u_1 \tag{18}$$

$$\dot{\delta}_B = \frac{1}{T_N}d_1 - \frac{1}{T_N}\delta_B + \frac{1}{T_N}u_1 + \frac{\alpha_3 V_3}{T_N} \tag{19}$$

Using the same technique to develop $\dot{d}_3$, $\dot{d}_4$, and $\dot{\delta}_C$ as was used to develop $\dot{d}_1$, $\dot{d}_2$, and $\dot{\delta}_B$, one obtains:

$$\dot{d}_3 = d_4 - \frac{16}{\tau}u_2 \tag{20}$$

$$\dot{d}_4 = \frac{-16}{\tau^2}d_3 - \frac{8}{\tau}d_4 + \frac{128}{\tau^2}u_2 \tag{21}$$

$$\dot{\delta}_C = \frac{1}{T_n}d_3 - \frac{1}{T_n}\delta_C + \frac{1}{T_n}u_2 + \frac{\alpha_4 V_4}{T_n} \tag{22}$$

Equations (1) - (5), (10) - (11), and (15) - (22) now constitiute the state description of the pilot-vehicle system.

F. DISPLAYED VARIABLES

The displayed variables listed below are those quantities which are assumed to be displayed or perceived by the pilot.

z_{p_1} ≈ Displayed Groundspeed Deviation = $K_1 u$

z_{p_2} ≈ Perceived Time Rate of Change of Glideslope Deviation = $K_2(-w + U_o \Theta)$

z_{p_3} ≈ Perceived Pitch Rate = $K_3 q$

z_{p_4} ≈ Displayed Pitch Angle Deviation = $K_4 \Theta$

z_{p_5} ≈ Displayed Glideslope Deviation = $K_5 h$

The K_i are display gains. For example:

$$K_3 = |K_3| \; \frac{\text{radians subtended at the pilot's eye by display}}{\text{rad/sec pitch}}$$

$$\frac{\text{element motion}}{\text{rate}}$$

Table 1 lists the display gains for this study.

According to modification (4) in section II.B., $\dot{u}$ should also be a perceived variable. However, since all perceived variables will be used in generating the director laws to be discussed, they must be measurable. If u represents airspeed, $\dot{u}$ will be difficult to sense. For this reason $\dot{u}$ was not considered a perceived variable (despite the fact the u represented groundspeed in this particular analysis).

It should be emphasized that neglecting $\dot{u}$ imposes little constraint on the model's validity since this variable is associated with the phugoid and will be quite small throughout the approach.

Display Gain	Value
K_1	3.44×10^{-4} rad/ft/sec
K_2	6.67×10^{-4} rad/ft/sec
K_3	9.55×10^{-2} rad/rad/sec
K_4	9.55×10^{-2} rad/rad/sec
K_5	6.67×10^{-4} rad/ft

TABLE I. Display Gains

G. OBSERVATION AND MOTOR NOISE

At present it is not possible to separate experimentally the various sources of pilot "remnant." In this paper, as is done in reference 2, observation noise and motor noise were taken to be representations of remnant. Observation noise was taken to be pilot injected noise in observing the displayed quantities, and motor noise was considered to be random error in control movement execution. Both were considered independent, Gaussian, white noise processes.

The pilot related noise levels were set at values considerably larger than those found in documented laboratory experiments (e.g. Ref. 2) so that the design would be less sensitive to pilot noise and more forgiving of actual non-optimal pilot behavior. Consequently, numerical values for

the observation noise and motor noise were chosen as $\rho = 0.1$, and $\rho' = .01$.

H. SYSTEM EQUATIONS AND MATRIX NOTATIONS

The system equations listed below define the optimal state-feedback controller and estimator problem. A thorough development of these equations can be found in reference 4.

$$\dot{\underline{x}}(t) = \underline{A}\ \underline{x}\ (t) + \underline{B}\ \underline{u}\ (t) + \underline{\gamma}\ \underline{w}\ (t) \tag{23}$$

$$\underline{y}(t) = \underline{C}\ \underline{x}\ (t) \tag{24}$$

$$\underline{z}(t) = \underline{H}\ \underline{x}\ (t) + \underline{v}\ (t) = \underline{z_p}\ (t) + \underline{v}\ (t) \tag{25}$$

$$E\left[w(t)w^T(T + \tau)\right] = F\ \delta(\tau) \tag{26}$$

$$E\left[v(t)v^T(T + \tau)\right] = \underline{G}\ \delta(\tau) \tag{27}$$

$$J = \lim_{T\to\infty} \frac{1}{T} \int_0^T \left[\underline{y}^T(t)\ \underline{Q}\ \underline{y}\ (t) + \underline{u}^T(t)\ \underline{R}\ \underline{u}\ (t)\right] dt \tag{28}$$

where

$\underline{A}$ is an n x n plant matrix

$\underline{x}(t)$ is an n x 1 state vector

$\underline{B}$ is an n x p control matrix

$\underline{u}(t)$ is a p x 1 control vector

$\underline{\gamma}$ is an n x t disturbance matrix

$\underline{w}(t)$ is a t x 1 disturbance vector

$\underline{y}(t)$ is a q x 1 output vector

$\underline{c}$ is a q x n output matrix

Here, $\underline{w}(t)$ is a vector of linearly uncorrelated, zero mean white noise signals with Gaussian amplitude probability

distribution functions. The elements of $\underline{w}(t)$ are assumed to be sample functions from n random processes which are each ergodic and are jointly ergodic. The covariance matrix for $\underline{w}(t)$ is

$$E\left[\underline{w}(t)\ \underline{w}^T(t+\tau)\right] = \underline{F}\ \delta(\tau) \tag{29}$$

where $\delta(\tau)$ is the unit impulse function.

The measured quantities on sensor signals are

$$\underline{z}(t) = \underline{H}\ \underline{w}(t) + \underline{v}\ (t) \tag{30}$$

where

$\underline{z}(t)$ is a u x 1 measurement vector

$\underline{H}$ is a u x n measurement matrix

$\underline{v}(t)$ is a u x 1 measurement noise vector

The elements of $\underline{v}(t)$ are assumed to be sample functions from p random processes each of which are ergodic and jointly ergodic. The covariance matrix for $\underline{v}(t)$ is

$$E\left[\underline{v}(t)\ \underline{v}^T(t+\tau)\right] = \underline{G}\ \delta(\tau) \tag{31}$$

The system is assumed to be completely controllable and completely observable. It is desired to find the control function $\underline{u}(t)$ which minimizes the quadratic scalar index of performance

$$J = \lim_{T\to\infty} \frac{1}{T} \int_0^T \left[\underline{y}^T(t)\ \underline{Q}\ \underline{y}(t) + \underline{u}^T(t)\ \underline{R}\ \underline{u}(t)\right] dt \tag{32}$$

where

$\underline{Q}$ is a q x q symmetric output cost weighting matrix and at least positive semidefinite

$\underline{R}$ is a p x p symmetric control cost weighting matrix and positive definite

The solution to the linear quadratic Gaussian control problem can be outlined as follows:

a.) The optimization problem can, by the called Separation Theorem, be broken up into two separate problems, an optimal control problem and an optimal estimation or filtering problem.

b.) The optimal estimation or filtering problem generates an optimal estimate, $\hat{\underline{x}}(t)$ of the state $\underline{x}(t)$. This estimate is optimal in the sense that

$$\lim_{T\to\infty} \frac{1}{T} \int_0^T \tilde{\underline{x}}^T(t)\, \tilde{\underline{x}}(t)\, dt$$

is minimized, where $\tilde{x}(t)$ is the estimation error defined as

$$\tilde{\underline{x}}(t) = \hat{\underline{x}}(t) - \underline{x}(t) \tag{33}$$

The optimal estimator (or Kalman filter) has the form

$$\dot{\hat{\underline{x}}}(t) = \underline{A}\,\hat{\underline{x}}(t) + \underline{B}\,\underline{u}(t) + \underline{K}\left[\underline{z}(t) - \underline{H}\,\hat{\underline{x}}(t)\right] \tag{34}$$

The estimator gains are given by

$$\underline{K} = \underline{P}\,\underline{H}^T\,\underline{G}^{-1} \tag{35}$$

where $\underline{P}$ is the error covariance matrix

$$E\left[\tilde{\underline{x}}(t)\tilde{\underline{x}}^T(t+\tau)\right] = \underline{P}\,\delta(t) \tag{36}$$

$\underline{P}$ is the positive definite solution to the steady - state filter matrix Riccati equation

$$\underline{A}\,\underline{P} + \underline{P}\,\underline{A}^T + \underline{\gamma}\,\underline{F}\,\underline{\gamma}^T - \underline{P}\,\underline{H}^T\,\underline{G}^{-1}\,\underline{H}\,\underline{P} = 0 \tag{37}$$

c.) The optimal control problem generates an optimal control law $\underline{u}(t)$ which is a linear function of the estimated state

$$\underline{u}(t) = - \underline{L}\, \hat{\underline{x}}(t) \tag{38}$$

where $\underline{L}$ is a p x n optimal controller gain matrix. The gain matrix $\underline{L}$ is identical to the one obtained by solving the optimal control problem with no system disturbance, exact state information, and the index of performance given by

$$J = \int_0^{\infty} \left[\underline{y}^T(t)\, \underline{Q}\, \underline{y}(t) + \underline{u}^T(t)\, \underline{R}\, \underline{u}(t) \right] dt \tag{39}$$

the controller gain matrix $\underline{L}$ is given by

$$\underline{L} = \underline{R}^{-1}\, \underline{B}^T\, \underline{S} \tag{40}$$

where $\underline{S}$ is the positive definite solution to the steady-state <u>control matrix Riccati equation</u>

$$- \underline{S}\, \underline{A} - \underline{A}^T\, \underline{S} - \underline{C}^T\, \underline{Q}\, \underline{C} + \underline{S}\, \underline{B}\, \underline{R}^{-1}\, \underline{B}^T\, \underline{S} = 0 \tag{41}$$

It can be shown that the state covariance matrix

$$E \left[\underline{x}(t)\, \underline{x}^T(t + \tau) \right] = (\underline{P} + \underline{M})\, \delta(t) \tag{42}$$

where $\underline{P}$ is the solution ot the filer matrix Riccati equation and $\underline{M}$ is the positive definite solution to

$$(\underline{A} - \underline{B}\, \underline{L})\, \underline{M} + \underline{M}\, (\underline{A} - \underline{B}\, \underline{L})^T + \underline{K}\, \underline{G}\, \underline{K}^T = 0 \tag{43}$$

In addition to the solutions outlined above, it can be shown that the transfer matrix relating the Laplace transform

of the optimal control law $\underline{u}(t)$ to the Laplace transform of the measurement vector $\underline{z}(t)$ (with $\underline{v}(t) \equiv 0$) is given by

$$\underline{U}(S) = -\underline{L}(S\underline{I} - \underline{A} + \underline{B}\,\underline{L} + \underline{K}\,\underline{H})^{-1}\underline{K}\,\underline{Z}(S) \tag{44}$$

where

$$\underline{U}(S) = \mathcal{L}\left[\underline{u}(t)\right] \tag{45}$$

$$\underline{Z}(S) = \mathcal{L}\left[\underline{z}(t)\right] \tag{46}$$

The state variables for this study were chosen in the following order

$$\begin{bmatrix} u \\ w \\ q \\ \Theta \\ h \\ w_g \\ u_g \\ d_1 \\ d_2 \\ \delta_B \\ d_3 \\ d_4 \\ \delta_C \end{bmatrix}$$

The following matrix tables were developed from equations (1) - (5), (10) - (11), and (17) - (22). The matrices are labeled in accordance with equations (23) - (27).

As Table VI indicates, all but one of the elements of $\underline{F}$ and $\underline{G}$ are dependent upon variances of system variables

which are not known a-priori. Estimates of these variances must be made, the solution to the optimal estimation and control problem obtained, and the resulting variances used in a second iteration. This iterative process continues until the equations for the α_i and V_{z_i} in Table VI are satisfied. As reference 2 points out, 2·m iterations are usually involved, where m is the number of displayed and perceived quantities.

The output vector $\underline{y}$ utilized in the index of performance is given in Table V as

$$\underline{y} = \begin{bmatrix} u \\ q \\ h \end{bmatrix}$$

The elements of the index of performance weighting matrices $\underline{Q}$ and $\underline{R}$ were chosen as the reciprocals of the "maximum allowable" deviations of the output and controls. Thus, when an output or control variable attains these subjectively chosen magnitudes, it makes a contribution of unity to the integrand of the index of performance. The maximum allowable deviations were chosen subjectively and varied with the flight conditions as Table V indicates.

A MATRIX

$$
\begin{bmatrix}
X_u & X_w & X_q & -g & 0 & -X_w & -X_u & 0 & 0 & X_{\delta_B} & 0 & 0 & X_{\delta_C} \\
Z_u & Z_w & U_o + Z_q & 0 & 0 & -Z_w & -Z_u & 0 & 0 & Z_{\delta_B} & 0 & 0 & Z_{\delta_C} \\
M_u+M_{\dot{w}}Z_u & M_w+M_{\dot{w}}Z_w & M_{\dot{w}}(U_o+Z_q)+M_q & 0 & 0 & -(M_w+M_{\dot{w}}Z_u) & -(M_u+M_{\dot{w}}Z_u) & 0 & 0 & M_{\delta_B}+M_{\dot{w}}Z_{\delta_B} & 0 & 0 & M_{\delta_C}+M_{\dot{w}}Z_{\delta_C} \\
0 & 0 & 1.0 & 0 & 0 & 0 & 0 & 0 & 0 & 0 & 0 & 0 & 0 \\
0 & -1.0 & 0 & U_o & 0 & 0 & 0 & 0 & 0 & 0 & 0 & 0 & 0 \\
0 & 0 & 0 & 0 & 0 & -\beta_1 & 0 & 0 & 0 & 0 & 0 & 0 & 0 \\
0 & 0 & 0 & 0 & 0 & 0 & 0 & -\beta_2 & 0 & 0 & 0 & 0 & 0 \\
0 & 0 & 0 & 0 & 0 & 0 & 0 & 0 & 0 & 0 & 0 & 0 & 0 \\
0 & 0 & 0 & 0 & 0 & 0 & 0 & -(\frac{16}{\tau^2}) & -\frac{8}{\tau} & 0 & 0 & 0 & 0 \\
0 & 0 & 0 & 0 & 0 & 0 & 0 & \frac{1}{T_N} & 0 & -\frac{1}{T_N} & 0 & 0 & 0 \\
0 & 0 & 0 & 0 & 0 & 0 & 0 & 0 & 0 & 0 & 0 & 0 & 0 \\
0 & 0 & 0 & 0 & 0 & 0 & 0 & 0 & 0 & 0 & \frac{-16}{\tau^2} & \frac{-8}{\tau} & 0 \\
0 & 0 & 0 & 0 & 0 & 0 & 0 & 0 & 0 & 0 & \frac{1}{T_N} & 0 & -\frac{1}{T_N}
\end{bmatrix}
$$

TABLE II

x Matrix B Matrix Y Matrix

$$
\begin{bmatrix} u \\ w \\ q \\ \Theta \\ h \\ w_g \\ u_g \\ d_1 \\ d_2 \\ \delta_B \\ d_3 \\ d_4 \\ \delta_C \end{bmatrix}
\qquad
\begin{bmatrix} 0 & 0 \\ 0 & 0 \\ 0 & 0 \\ 0 & 0 \\ 0 & 0 \\ 0 & 0 \\ 0 & 0 \\ \frac{-16}{\tau} & 0 \\ \frac{128}{\tau^2} & 0 \\ \frac{1}{T_N} & 0 \\ 0 & \frac{-16}{\tau} \\ 0 & \frac{128}{\tau^2} \\ 0 & \frac{1}{T_N} \end{bmatrix}
\qquad
\begin{bmatrix} 0 & 0 & 0 & 0 \\ 0 & 0 & 0 & 0 \\ 0 & 0 & 0 & 0 \\ 0 & 0 & 0 & 0 \\ 0 & 0 & 0 & 0 \\ 1.0 & 0 & 0 & 0 \\ 0 & 1.0 & 0 & 0 \\ 0 & 0 & 0 & 0 \\ 0 & 0 & 0 & 0 \\ 0 & 0 & \frac{1}{T_N} & 0 \\ 0 & 0 & 0 & 0 \\ 0 & 0 & 0 & 0 \\ 0 & 0 & 0 & \frac{1}{T_N} \end{bmatrix}
$$

TABLE III.

H Matrix

$$
\begin{bmatrix}
K_1 & 0 & 0 & 0 & 0 & 0 & -K_oK_1 & 0 & 0 & 0 & 0 & 0 & 0 \\
0 & -K_2 & 0 & K_2U_o & 0 & 0 & 0 & 0 & 0 & 0 & 0 & 0 & 0 \\
0 & 0 & K_3 & 0 & 0 & 0 & 0 & 0 & 0 & 0 & 0 & 0 & 0 \\
0 & 0 & 0 & K_4 & 0 & 0 & 0 & 0 & 0 & 0 & 0 & 0 & 0 \\
0 & 0 & 0 & 0 & K_5 & 0 & 0 & 0 & 0 & 0 & 0 & 0 & 0
\end{bmatrix}
$$

TABLE IV.

y Matrix

C Matrix

$$\begin{bmatrix} y_1 \\ y_2 \\ y_3 \end{bmatrix} = \begin{bmatrix} 1 & 0 & 0 & 0 & 0 & 0 & 0 & 0 & 0 & 0 & 0 & 0 & 0 \\ 0 & 0 & 1 & 0 & 0 & 0 & 0 & 0 & 0 & 0 & 0 & 0 & 0 \\ 0 & 0 & 0 & 0 & 1 & 0 & 0 & 0 & 0 & 0 & 0 & 0 & 0 \end{bmatrix}$$

20 Knots

$u_{max} = 3$ ft/sec

$q_{max} = .04$ rad/sec

$h_{max} = 5$ ft

$\delta_B = .25$ ft

$\delta_C = .25$ ft

Q Matrix

$$\begin{bmatrix} \left(\frac{1}{u_{max}}\right)^2 & 0 & 0 \\ 0 & \left(\frac{1}{q_{max}}\right)^2 & 0 \\ 0 & 0 & \left(\frac{1}{h_{max}}\right)^2 \end{bmatrix}$$

R Matrix

$$\begin{bmatrix} \left(\frac{1}{\delta_{B_{max}}}\right)^2 & 0 \\ 0 & \left(\frac{1}{\delta_{C_{max}}}\right)^2 \end{bmatrix}$$

40 Knots

$u_{max} = 7$ ft/sec

$q_{max} = .04$ rad/sec

$h_{max} = 10$ ft

$\delta_{B_{max}} = .25$ ft

$\delta_{C_{max}} = .25$ ft

60 Knots

$u_{max} = 10$ ft/sec

$q_{max} = .04$ rad/sec

$h_{max} = 10$ ft

$\delta_{B_{max}} = .25$ ft

$\delta_{C_{max}} = .25$ ft

TABLE V.

w Matrix

$$\begin{bmatrix} w_1 \\ w_2 \\ w_3 \\ w_4 \end{bmatrix}$$

F Matric

$$\begin{bmatrix} \alpha_1^2 & 0 & 0 & 0 \\ 0 & \alpha_2^2 & 0 & 0 \\ 0 & 0 & \alpha_3^2 & 0 \\ 0 & 0 & 0 & \alpha_4^2 \end{bmatrix}$$

$$\alpha_1 = \left[\frac{2U_o}{L_w}\right]^{\frac{1}{2}} \sigma_w$$

$$\alpha_2 = \left[\frac{2U_o}{L_u}\right]^{\frac{1}{2}} \sigma_u$$

$$\alpha_3 = \left[\rho' \cdot \pi \cdot E\left[u_1^2(t)\right]\right]^{\frac{1}{2}}$$

$$\alpha_4 = \left[\rho' \cdot \pi \cdot E\left[u_2^2(t)\right]\right]^{\frac{1}{2}}$$

v Matrix

$$\begin{bmatrix} v_1 \\ v_2 \\ v_3 \\ v_4 \\ v_5 \end{bmatrix}$$

G Matrix

$$\begin{bmatrix} V_{z_1} & 0 & 0 & 0 & 0 \\ 0 & V_{z_2} & 0 & 0 & 0 \\ 0 & 0 & V_{z_3} & 0 & 0 \\ 0 & 0 & 0 & V_{z_4} & 0 \\ 0 & 0 & 0 & 0 & V_{z_5} \end{bmatrix}$$

$$V_{z_1} = \rho \cdot \pi \cdot E\left[z_{p_1}^2(t)\right]$$

$$V_{z_2} \quad \rho \cdot \pi \cdot E\left[z_{p_2}^2(t)\right]$$

$$V_{z_3} \quad \rho \cdot \pi \cdot E\left[z_{p_3}^2(t)\right]$$

$$V_{z_4} \quad \rho \cdot \pi \cdot E\left[z_{p_4}^2(t)\right]$$

$$V_{z_5} \quad \rho \cdot \pi \cdot E\left[z_{p_5}^2(t)\right]$$

TABLE VI.

III. PILOT MODELING EXAMPLE

This section presents a numerical illustration of the pilot modeling technique developed in Section H. The longitudinal dynamics of a UH-1H helicopter at an approach groundspeed of 60 knots are utilized. The normalized UH-1H longitudinal derivatives, in a stability axis system, are shown in Table VII.

A modified form of the Variable Automatic Synthesis Program (VASP) /Ref. 5/ was utilized to solve the optimal estimation and control problem. The solution to this problem constitutes the pilot-vehicle model. After roughly 10 iterations the solution for the 60-knot case converged. Table VIII shows the root-mean-square (RMS) performance figures. The ten pilot transfer functions relating the cyclic and collective control variables to the five displayed and perceived quantities were obtained. Figures 3 and 4 are Bode plot representations for the $\frac{\delta_B}{u}(s)$ and $\frac{\delta_C}{\dot{h}}(s)$ pilot transfer functions respectively.

Pure gain approximations were then made to each of the transfer functions in the frequency range of interest for modeling purposes: $.1 < \omega <$ rad/sec. The gains were then normalized by dividing by the magnitude of the largest gain for each control. The values in Table IX resulted. For example, using the gains of Table IX the cyclic and collective flight director laws become

$$\dot{\delta}_B(t) = -8.42 \cdot 10^{-4} u(t) - 2.45 \cdot 10^{-4} \dot{h}(t) + q(t)$$

$$+ .1945\, \Theta(t) - 4.02 \cdot 10^{-4} h(t) \qquad (47)$$

$$\dot{\delta}_C(t) = 2.47 \cdot 10^{-4} u(t) - 5.52 \cdot 10^{-3} \dot{h}(t) - q(t)$$

$$- .1358\, \Theta(t) + 1.96 \cdot 10^{-3} h(t) \qquad (48)$$

where δ_B' and δ_C' are the cyclic and collective director signals respectively.

TABLE VII.

The NORMALIZED UH-1H LONGITUDINAL DERIVATIVES IN STABILITY AXIS SYSTEM

U_o	=	0.10134E 03	ft/sec
X_u	=	-0.34137E-01	1/sec
X_w	=	0.19899E-01	1/sec
X_q	=	0.15661E 02	ft/sec
Z_u	=	-0.49388E-01	1/sec
Z_w	=	-0.89470E 00	1/sec
Z_q	=	0.36540E 02	ft/sec
M_u	=	0.14837E-02	1/sec-ft
M_w	=	-0.12117E-01	1/sec-ft
M_q	=	-0.28505E 01	1/sec
$M_{\dot{w}}$	=	0.0	1/ft
X_{δ_B}	=	0.80591E 01	1/sec-sec
X_{δ_C}	=	-0.32832E 00	1/sec-sec
Z_{δ_B}	=	0.22374E 02	1/sec-sec
Z_{δ_C}	=	-0.11944E 03	1/sec-sec
M_{δ_B}	=	-0.25335E 01	1/ft-sec-sec
M_{δ_C}	=	0.71803E 00	1/ft-sec-sec

RMS		Performance
$\sqrt{\bar{u}^2(t)}$	=	3.03 ft/sec
$\sqrt{\bar{w}^2(t)}$	=	5.11 ft/sec
$\sqrt{\bar{q}^2(t)}$	=	1.01 degree/sec
$\sqrt{\bar{\theta}^2(t)}$	=	1.46 degree
$\sqrt{\bar{h}^2(t)}$	=	9.32 ft
$\sqrt{\bar{w}_g^2(t)}$	=	5 ft/sec
$\sqrt{\bar{u}_g^2(t)}$	=	5 ft/sec
$\sqrt{\bar{\delta}_g^2(t)}$	=	1.12 in
$\sqrt{\bar{\delta}_C^2(t)}$	=	1.35 in

TABLE VIII.

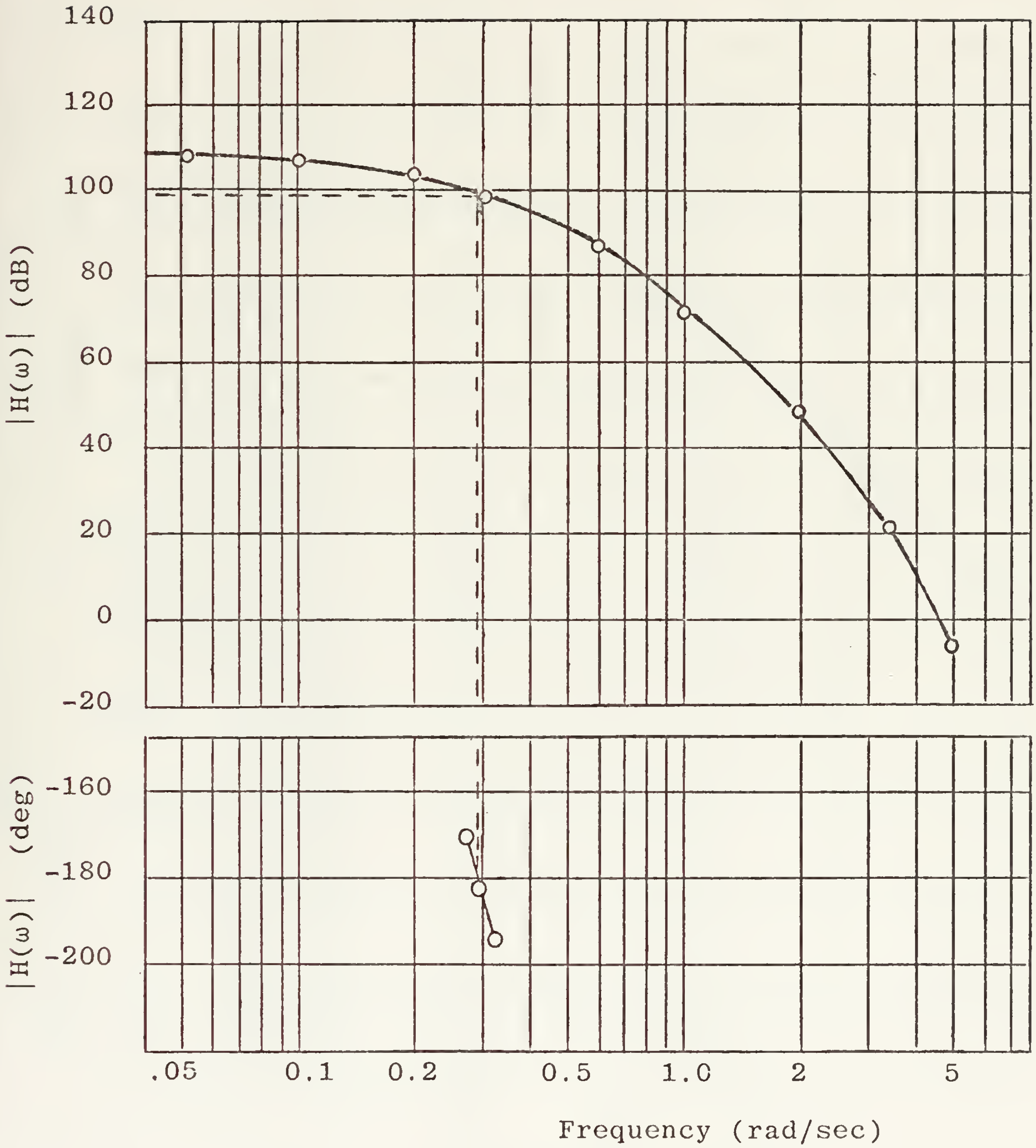

FIGURE 3. TRANSFER FUNCTION $\frac{\delta_B}{u}$ (S)

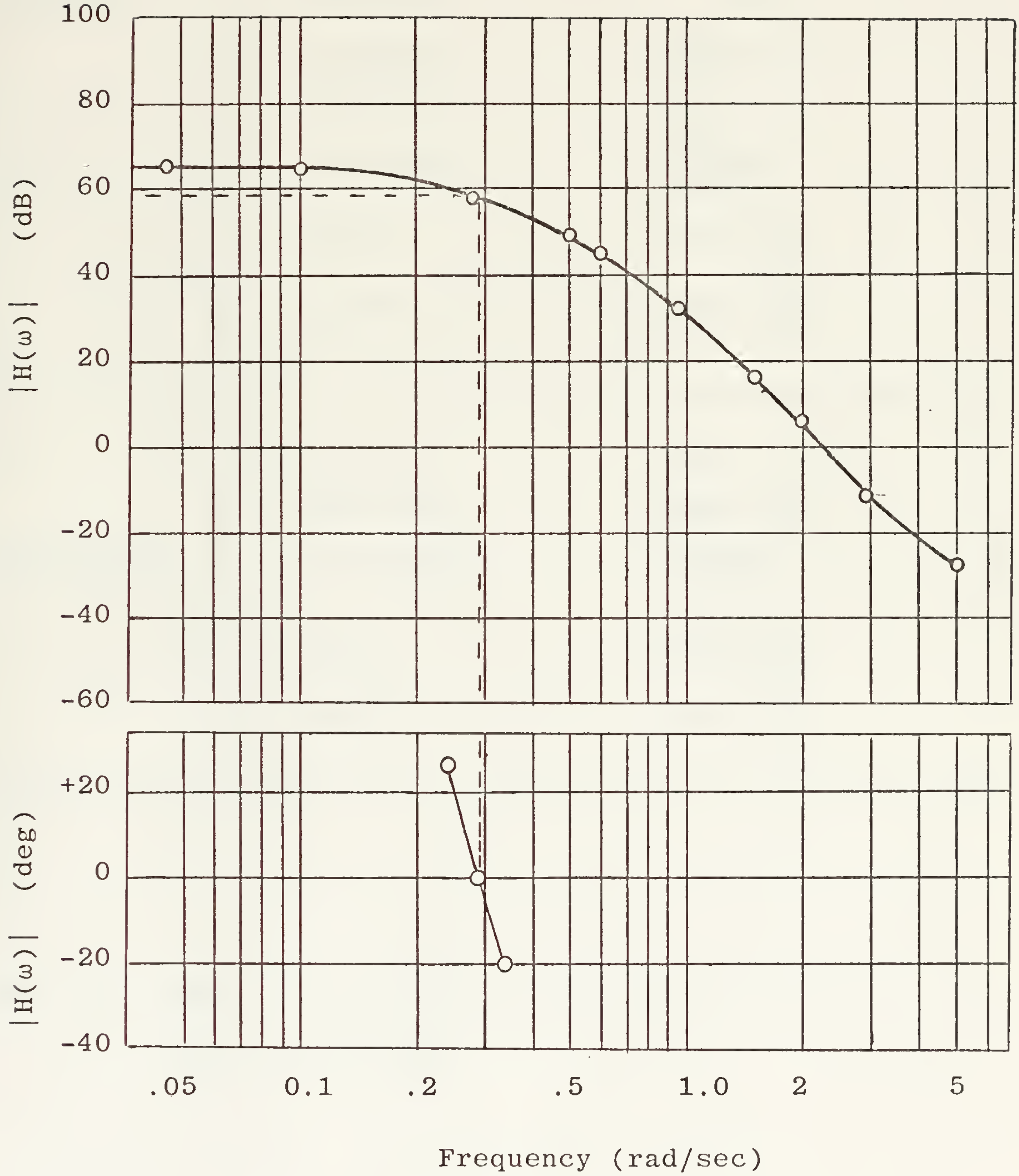

FIGURE 4, TRANSFER FUNCTION $\frac{\delta_C}{\dot{h}}$ (S)

DIRECTOR	SENSORY VARIABLE	LOW-FREQUENCY GAIN
CYCLIC	Airspeed	$-.000842$ sec
	Sink Rate	$-.000245$ sec
	Pitch Rate	$1 \frac{\text{ft-sec}}{\text{rad}}$
	Pitch	$.1945 \frac{\text{ft}}{\text{rad}}$
	Height	$-.000402 \frac{\text{ft}}{\text{ft}}$
COLLECTIVE	Airspeed	$.000247$ sec
	Sink Rate	$.00552$ sec
	Pitch Rate	$-1 \frac{\text{ft-sec}}{\text{rad}}$
	Pitch	$-.1358 \frac{\text{ft}}{\text{rad}}$
	Height	$.00196 \frac{\text{ft}}{\text{ft}}$

TABLE IX. Gains for UH-1H Helicopter Director Laws - Velocity 60 Knots

IV. RESULTS AND CONCLUSIONS

The normalized director gains for the 40 and 20-knot approach speeds are shown in the following tables. It should be noted that all of the Bode magnitude plots for the thirty pilot transfer functions (ten each for each of the three approach speeds) could be approximated by a fifth-order low pass filter. The break frequency varied somewhat between 0.4 and 0.5 rad/sec. Only the director control gain changed from function to function.

In order to ascertain the reason for the rather dramatic sign reversals which occurred in some of the larger gains as the flight condition changed (e.g. in the collective-to-pitch rate and collective-to-pitch gains of Table IX and Table X), the author re-ran the 40-knot case with identical pilot parameters, specifically $\underline{Q}$ and $\underline{R}$ matrices, as in the 60-knot case. The results were similar to those of Table X. This indicated that the flight condition dictated the gain sign variation and not the subjective selection of the $\underline{Q}$ and $\underline{R}$ matrices in the pilot model.

The director laws implicit in Tables IX - XI must be evaluated in piloted simulation before the efficiency of the design method outlined in this thesis can be determined.

DIRECTOR	SENSORY VARIABLE	LOW-FREQUENCY GAIN
CYCLIC	Airspeed	.000536 sec
	Sink Rate	-.005287 sec
	Pitch Rate	1.0 $\frac{\text{ft-sec}}{\text{rad}}$
	Pitch	.374 $\frac{\text{ft}}{\text{rad}}$
	Height	-.00175 $\frac{\text{ft}}{\text{ft}}$
COLLECTIVE	Airspeed	.000426 sec
	Sink Rate	-.0044 sec
	Pitch Rate	1.0 $\frac{\text{ft-sec}}{\text{rad}}$
	Pitch	.41962 $\frac{\text{ft}}{\text{rad}}$
	Height	-.00188 $\frac{\text{ft}}{\text{ft}}$

TABLE X. Gains for UH-1H Helicopter Director Laws - Velocity 40 Knots.

DIRECTOR	SENSORY VARIABLE	LOW-FREQUENCY GAIN
CYCLIC	Airspeed	-.0126 sec
	Sink Rate	.004448 sec
	Pitch Rate	$1 \frac{\text{ft-sec}}{\text{rad}}$
	Pitch	$.277 \frac{\text{ft}}{\text{rad}}$
	Height	$.00259 \frac{\text{ft}}{\text{ft}}$
COLLECTIVE	Airspeed	-.01257 sec
	Sink Rate	.00435 sec
	Pitch Rate	$1 \frac{\text{ft-sec}}{\text{rad}}$
	Pitch	$.3005 \frac{\text{ft}}{\text{rad}}$
	Height	$.002535 \frac{\text{ft}}{\text{ft}}$

TABLE XI. Gains for UH-1H Helicopter Director Laws - Velocity 20 Knots.

LIST OF REFERENCES

1. Levison, W.H, "A Model-Based Technique for the Design of Flight-Directors," Proc. 9th Annual Conf. Manual Control, pp. 163-172, May 1973.

2. Kleinman, D.L., Baron, S., Levison, W.H., "An Optimal Control Model of Human Response Part I: Theory and Validation," Automatica, Vol. 6, pp. 357-369.

3. Hart, J.E., Lowry, A.A., Lacau, L.L., "Stochastic Disturbance Data for Flight Control System Analysis," Technical Documentary Report No. ASD-TDR-62-347, September 1962.

4. Bryson, A.E, Ho, Yu-Chi, Applied Optimal Control, Ginn and Company, 1969.

5. NASA Ames Research Center Report TMX-2417, Users Manual for the Variable Dimension Automatic Synthesis Program (VASP, by J.S. White and H.Q. Lee, October 1971.

INITIAL DISTRIBUTION LIST

		No. Copies
1.	Defense Documentation Center Cameron Station Alexandria, Virginia 22314	2
2.	Library, Code 0212 Naval Postgraduate School Monterey, California 93940	2
3.	Chairman Department of Aeronautical Engineering Naval Postgraduate School Monterey, California 93940	2
4.	Asst. Professor Ronald A. Hess 57He Department of Aeronautical Engineering Naval Postgraduate School Monterey, California 93940	1
5.	Lt. G. K. Smith, USN 786 Tonga Court San Jose, California 95127	1

160740
Thesis
S5779 Smith
c.1
Flight director laws
for the longitudinal
cyclic and collective
controls of the UH-1H
helicopter.